Desalination and Water Treatment
www.deswater.com
doi: 10.1080/19443994.2012.751882

51 (2013) 4573–4581
June

Taylor & Francis
Taylor & Francis Group

Color removal from aqueous solutions of metal-containing dye using pine cone

Fatih Deniz

Nigar Erturk Trade Vocational High School, Gaziantep 27590, Turkey
Tel. +90 342 3291194; Fax: +90 342 3291529; email: f_deniz@windowslive.com

Received 5 September 2012; Accepted 19 November 2012

ABSTRACT

The ability of pine cone (PC) for dye removal from aqueous media was studied and Lanasol Yellow 2R (LY2R) was used as a model metal-containing dye. The effects of various parameters like pH, adsorbent dosage and size, dye concentration, temperature, contact time and ionic strength on the dye adsorption were investigated. The equilibrium data were well represented by the Langmuir isotherm model. The maximum adsorption capacity of the PC for LY2R was found as 41.15 mg g^{-1}. The adsorption kinetics followed the pseudo-second-order model. The thermodynamic tests revealed that the adsorption was spontaneous and endothermic process. Accordingly, the PC could be employed as a promising alternative adsorbent for eliminating the dye from aqueous solutions.

Keywords: Metal-containing dye; Adsorption; Pine cone; Color removal

1. Introduction

Metal-containing dyes are widely used in the textile and leather tanning industries for dyeing protein and polyamide fibers due to their excellent light fastness [1]. Generally, these dyes are chromium, cobalt and copper complexes. They are resistant to biological activity, light and other environmental conditions because of their complex aromatic structures. The metal-containing dyes are toxic and potentially carcinogenic, and have caused serious environmental pollutions [2]. Therefore, an economical and eco-friendly method is needed for the treatment of such dyes. Among the various methods for the dye removal, adsorption process is one of the most efficient techniques due to its simplicity of design, ease of operation and insensitivity to toxic substances [3]. Although commercial activated carbon is a preferred adsorbent due to large surface area, micro-porous structure and high adsorption capacity, its widespread use is limited because of high capital and regeneration cost [4]. Thus, there is a growing interest in finding alternative low-cost adsorbents for the dye removal. Though many studies have been made in this aim, the reports on the adsorption of metal-containing dyes are very limited.

In recent years, it has been shown that agro-forest lingo-cellulosic residues have good adsorption capacities for some dyes and metals [4]. Female cones from conifer trees, which are abundant in the wood processing fields and may constitute another promising lingo-cellulosic adsorbent, have been applied more recently for adsorption of various metals and dyes [5,6]. However, their potentialities for the metal-containing dyes have been almost unexplored. The utilizes of conifer cones have been limited to domestic fuel in some rural areas, extraction of essential oils for

therapeutic purposes when they are still unripe, and on seasonal decoration [5]. Thus, such new uses of the conifer cones can provide additional income for the forest landowners.

The aim of present work was to examine the feasibility of natural pine cone (PC) as an adsorbent due to its low-cost, high efficiency and ready availability for the removal of Lanasol Yellow 2R (LY2R) as a model metal-containing dye from aqueous solutions in batch mode. The effects of various operational parameters on the dye removal were examined. The equilibrium, kinetic and thermodynamic parameters were obtained from the applications of various mathematical models.

2. Materials and methods

2.1. Preparation of PC adsorbent and LY2R solution

The PC used in this study was collected from the forest of Burc, Gaziantep and Turkey. It was firstly washed with distilled water, dried at 70°C for 24 h, crushed in a domestic grinder and sieved to obtain particle size in the range of 63–500 μm. The powdered adsorbent was stored in an airtight container until use. No other chemical or physical treatment was used prior to adsorption experiments.

LY2R dye was supplied by a local textile factory and used without further purification. The dye was of commercial purity. The chemical structure and some properties of LY2R are given in Fig. 1 and Table 1, respectively. A stock solution of 500 mg L^{-1} was prepared by dissolving accurate quantity of the dye in distilled water. The test solutions were prepared by diluting the stock solution to the required concentrations. Fresh dilutions were used for each experiment. 0.1 M NaOH and 0.1 M HCl solutions were used for initial pH adjustment.

2.2. Batch adsorption studies

The experiments were carried out with the PC in 100 mL conical flasks containing 50 mL LY2R solutions in a water bath to evaluate the experimental parameters such as pH (pH, 2–10), adsorbent dosage

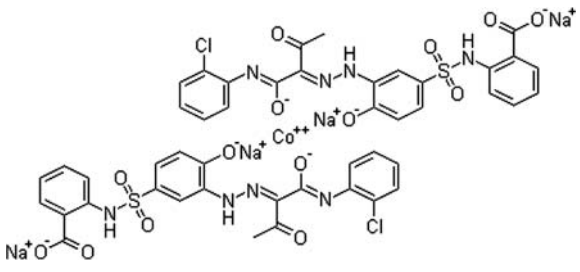

Fig. 1. Molecular structure of LY2R dye.

Table 1
Some properties of LY2R dye

CI name	Acid Yellow 220
Synonyms	Irgasperse Yellow 2R, Ostalan Yellow S-G
Molecular formula	$C_{46}H_{32}C_{l2}CoN_8Na_4O_{14}S_2$
Molar mass	1206.72 g mol^{-1}
CI number	11714
CAS number	70851-34-2
Type	Anionic
Maximum absorbance	420 nm

(m, 1–6 g L^{-1}), adsorbent size (d_p, 63–500 μm), dye concentration (C_o, 20–100 mg L^{-1}), temperature (T, 25–45°C), contact time (t, 0–120 min) and ionic strength (I_s, 0.1–0.5 mol L^{-1}). After each adsorption run, the samples were centrifuged (5,000 rpm, 10 min) for solid–liquid separation and the residual dye concentration in the solutions was analysed by a UV–vis spectrophotometer at 420 nm. The equilibrium, kinetic and thermodynamic studies were performed at the same adsorption conditions.

The amount of dye adsorbed onto adsorbent (q, mg g^{-1}) and the percentage of dye removal efficiency (R,%) were calculated by Eqs. (1) and (2), respectively.

$$q = \frac{(C_o - C_r)V}{M} \tag{1}$$

$$R(\%) = \frac{C_o - C_r}{C_o} \times 100 \tag{2}$$

where C_o is the initial dye concentration (mg L^{-1}), C_r is the residual dye concentration at any time (mg L^{-1}), V is the volume of solution (L) and M is the mass of adsorbent (g). q and C_r are equal to q_e and C_e at equilibrium, respectively.

2.3. Characterization of PC

To obtain a qualitative and preliminary analysis of the main functional groups that might be involved in the dye uptake, the Fourier transform infrared (FTIR) analysis of PC was performed using a FTIR spectrometer (PerkinElmer, Spectrum 100) in the range of 650–4000 cm^{-1}. A scanning electron microscope (SEM) (JEOL, JSM-6390LV) was used to obtain information about the surface morphological structure of PC.

2.4. Statistical tests

The adsorption studies were performed in duplicates for ensuring the reliability and reproducibility of

the results obtained and only the mean values were reported. All the model parameters were determined by linear regression, using the Excel 2010 program (Microsoft Co., USA). In addition to the coefficient of determination (R^2), the Chi-square (χ^2) statistical test method was also used to evaluate the best-fit of the model to the experimental data using Eq. (3).

$$\chi^2 = \sum_{i=1}^{n} \frac{(q_{e,exp} - q_{e,cal})^2}{q_{e,cal}} \quad (3)$$

where n is the number of data points, $q_{e,exp}$ is the observation from the experiment and $q_{e,cal}$ is the calculation from the models. The smaller χ^2 value denotes the best curve fitting.

3. Results and discussion

3.1. Properties of PC

PC is composed of epidermal and sclerenchyma cells which contain cellulose, hemicelluloses, lignin, rosin and tannins in their cell walls which contain polar functional groups such as alcohols, aldehydes, ketones, carboxylic, phenolic and other groups. These groups will form active sites for adsorption on the material surface [7]. The FTIR spectrum of PC is shown in Fig. 2. The pick positions defined for PC and other characteristics of PC [7,8] are presented in Table 2. These picks indicated that PC is composed of various functional groups which are responsible for the binding of LY2R dye.

The surface morphology of PC obtained by the SEM is given in Fig. 3. The PC is made up of a rough multilayer surface. This surface can be seen to contain small pores indicating that this material presents good characteristics to be employed as a natural adsorbent for the dye uptake. It is believed that these pores provide ready access and large surface area for the adsorption of dye on the binding sites [9].

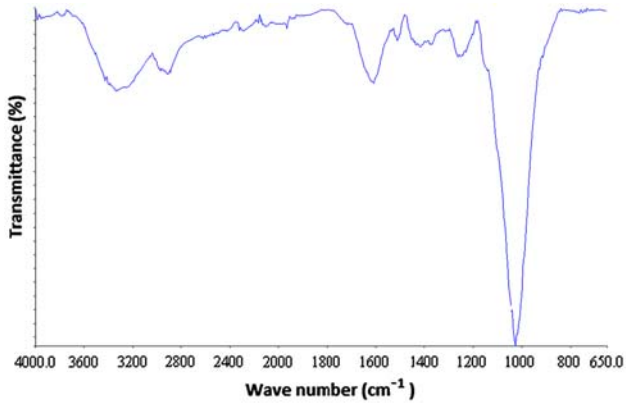

Fig. 2. FTIR spectrum of PC.

Table 2
General characteristics of PC

Hemicellulose	46.5%
Cellulose	18.8%
Lignin	37.4%
Extractive	15.4%
BET surface area	4.4 $m^2 g^{-1}$
Iodine number	15.5 mg g^{-1}
Total basicity	4.3 mmol g^{-1}
Point zero charge	7.5
Functional groups	
O–H	3336.3 cm^{-1}
C–H	2908.7 cm^{-1}
C=O	1604.8 cm^{-1}
C–N	1245.1 cm^{-1}
–C–C–	1025.2 cm^{-1}
–CN	770.5 cm^{-1}

3.2. Effects of process parameters on adsorption

The solution pH affects not only the surface charge of adsorbent molecule, the degree of ionization of the materials and the dissociation of functional groups on the active sites of the adsorbent, but also the structure of the dye molecule. The results of pH studies are shown in Fig. 4 (m: 1 g L^{-1}, d_p: 63–125 μm, C_o: 40 mg L^{-1}, T: 25°C and t: 75 min). It is evident that the LY2R adsorption is higher at lower pH and as the pH of solution increases, it decreases sharply. The lower adsorption at alkaline pH could be attributed to the abundance of hydroxyl ions which will compete with the dye anions for the same adsorption sites [10].

The adsorbent dose is an important parameter in the adsorption studies because it gives an idea of the adsorbent efficiency. It was observed that percentage of dye removal increased with increase of adsorbent dosage (Fig. 5) (pH: 4, d_p: 63–125 μm, C_o: 40 mg L^{-1}, T: 25°C and t: 75 min). Such a trend is mostly attributed to an increase in the adsorptive surface area and the availability of more active adsorption sites [11]. The adsorbent particle size is another significant factor on the adsorption process. For this work, the results let to the conclusion that the dye adsorption increased with decreasing particle size (Fig. 6) (pH: 4, m: 1 g L^{-1}, C_o: 40 mg L^{-1}, T: 25°C and t: 75 min). This may be due to the fact that the smaller adsorbent particles have shortened diffusion paths, such that the ability of dye to penetrate all internal pores of the adsorbent is higher [11].

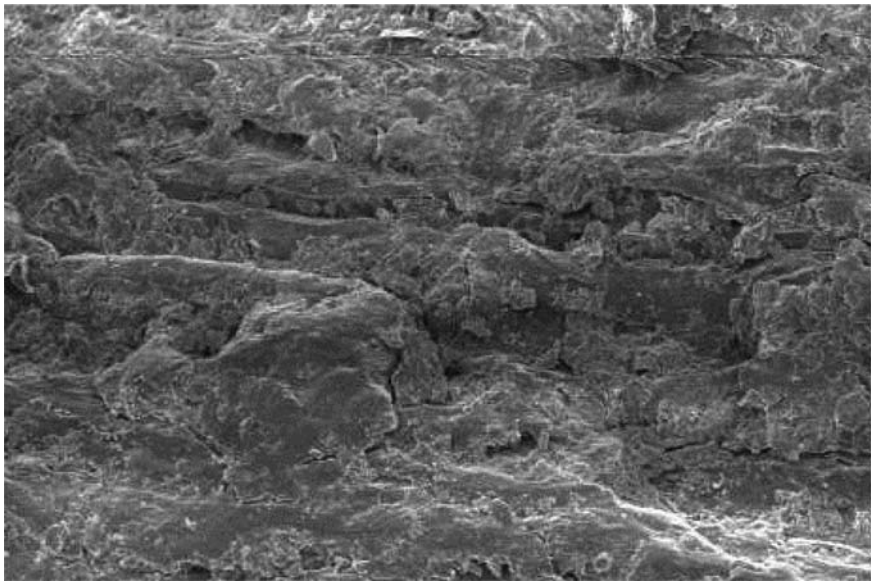

Fig. 3. SEM image of PC (3.0 kV, X430).

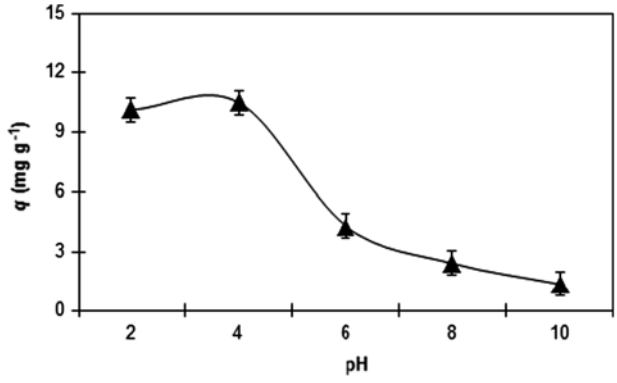

Fig. 4. Effect of pH.

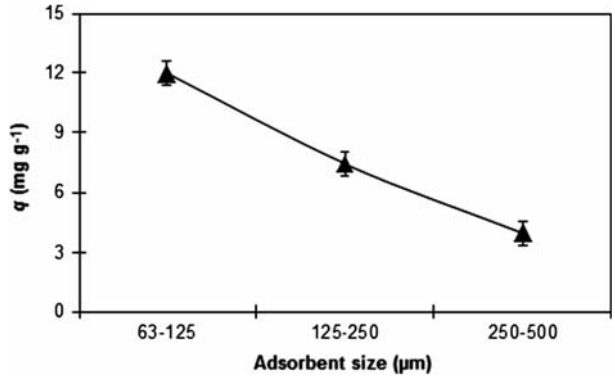

Fig. 6. Effect of particle size.

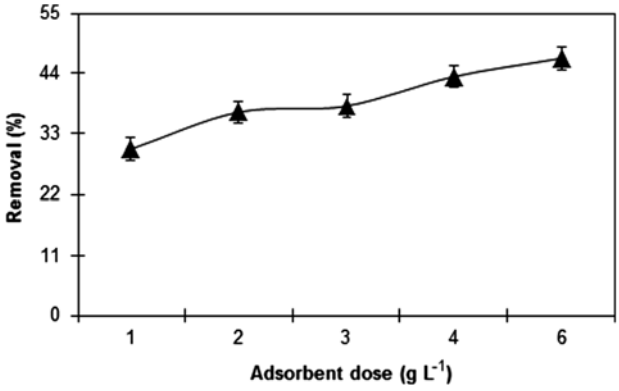

Fig. 5. Effect of adsorbent dose.

The dye concentration has an apparent influence on its removal from aqueous phase. The effect of LY2R concentration on the efficiency of adsorption was investigated in the initial concentration range of 20–100 mg L^{-1} (Fig. 7) (pH: 4, m: 1 g L^{-1}, d_p: 63–125 µm, T: 25°C, t: 75 min). The adsorption capacity of PC increased from 6.24 to 23.53 mg g^{-1} with increase in the initial dye concentration from 20 to 100 mg L^{-1}. This trend may be due to the high driving force for mass transfer at a high initial dye concentration. In addition, if the dye concentration in solution is higher, the active sites of adsorbent are surrounded by much more dye molecules, and the adsorption phenomenon occurs more efficiently. Thus, adsorption amount increases with the increase of initial dye concentration [12].

The temperature is a significant controlling factor in the real applications of adsorbent for the dye removal process. The effect of temperature on the adsorption of LY2R by the adsorbent was studied in

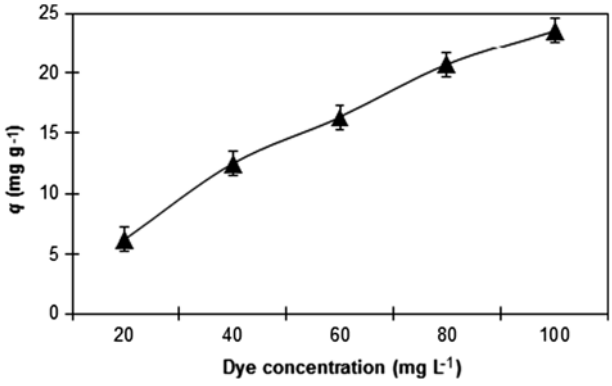

Fig. 7. Effect of dye concentration.

the range of 25–45˚C and the results are presented in Fig. 8 as a function of contact time (pH: 4, m: 1 g L^{-1}, d_p: 63–125 μm, C_o: 100 mg L^{-1}). The dye removal increased from 23.16 to 34.89 mg g^{-1} with the rise in temperature from 25 to 45˚C, suggesting that the process was endothermic in nature. The better adsorption at higher temperature may be due to enhanced mobility of the dye molecules from the solution to the adsorbent surface [13]. Besides, the dye adsorption was rapid in the initial stages of removal process and increased with an increase in contact time up to 120 min. After this period, the adsorption amount did not significantly change. The fast initial adsorption rate may be attributed to a large number of the vacant dye-binding sites being available for adsorption during the initial stage. At higher contact time, the rate of adsorption inclined to slow down, gradually leading to equilibrium. This trend could be referred to the decrease in the number of vacant sites being available for further dye removal [12]. The short equilibrium time points out the efficiency and applicability of adsorbent for real wastewater treatment process.

The occurrence of various types of salts is rather common in colored effluents. The salts could change the ionic nature, hydrophobicity, size and solubility of

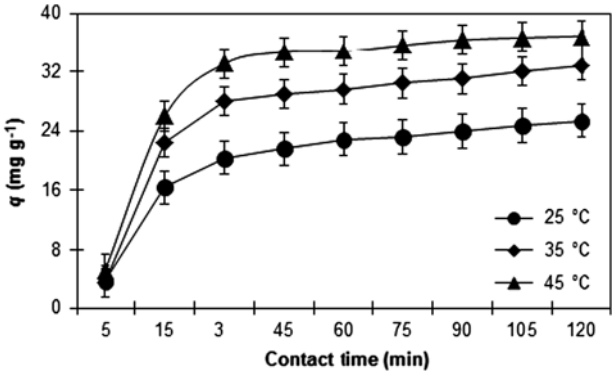

Fig. 8. Effect of contact time and temperature.

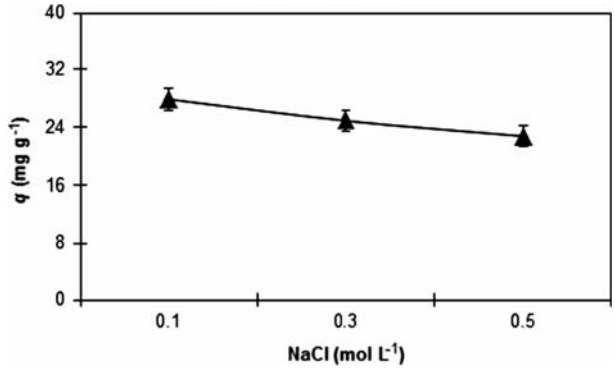

Fig. 9. Effect of ionic strength.

the dye, and their presence leads to high ionic strength, which may significantly affect the performance of dye adsorption process [14]. In this study, sodium chloride (0.1–0.5 mol L^{-1}) was used to simulate the ionic strength of salt in colored wastewaters. The increased ionic strength led to a decrease in the dye adsorption potential of adsorbent (Fig. 9) (pH: 4, m: 1 g L^{-1}, d_p: 63–125 μm, C_o: 100 mg L^{-1}, T: 25˚C and t: 60 min). This phenomenon may be explained by the possibility of ion exchange mechanism or the competition between chloride anions and negatively charged dye molecules for the same binding sites.

3.3. Equilibrium researches

The isotherm studies are very important for the optimization of adsorption process. In this research, the equilibrium data were analysed by the most commonly used isotherm models; Langmuir, Freundlich, Dubinin–Radushkevich (D-R) and Temkin.

The linear form of theLangmuir equation can be given as [15]:

$$\frac{C_e}{q_e} = \frac{1}{bq_m} + \frac{C_e}{q_m} \quad (4)$$

where q_e is the amount of dye adsorbed onto adsorbent at equilibrium, b is the Langmuir constant and q_m is the monolayer adsorption capacity. The values of b and q_m can be calculated from the slope and intercept of the plots between C_e/q_e and C_e, respectively (Fig. 10(A)).

The essential feature of the Langmuir isotherm can be expressed in terms of the dimensionless separation parameter, R_L, defined as [16]:

$$R_L = \frac{1}{1 + bC_o} \quad (5)$$

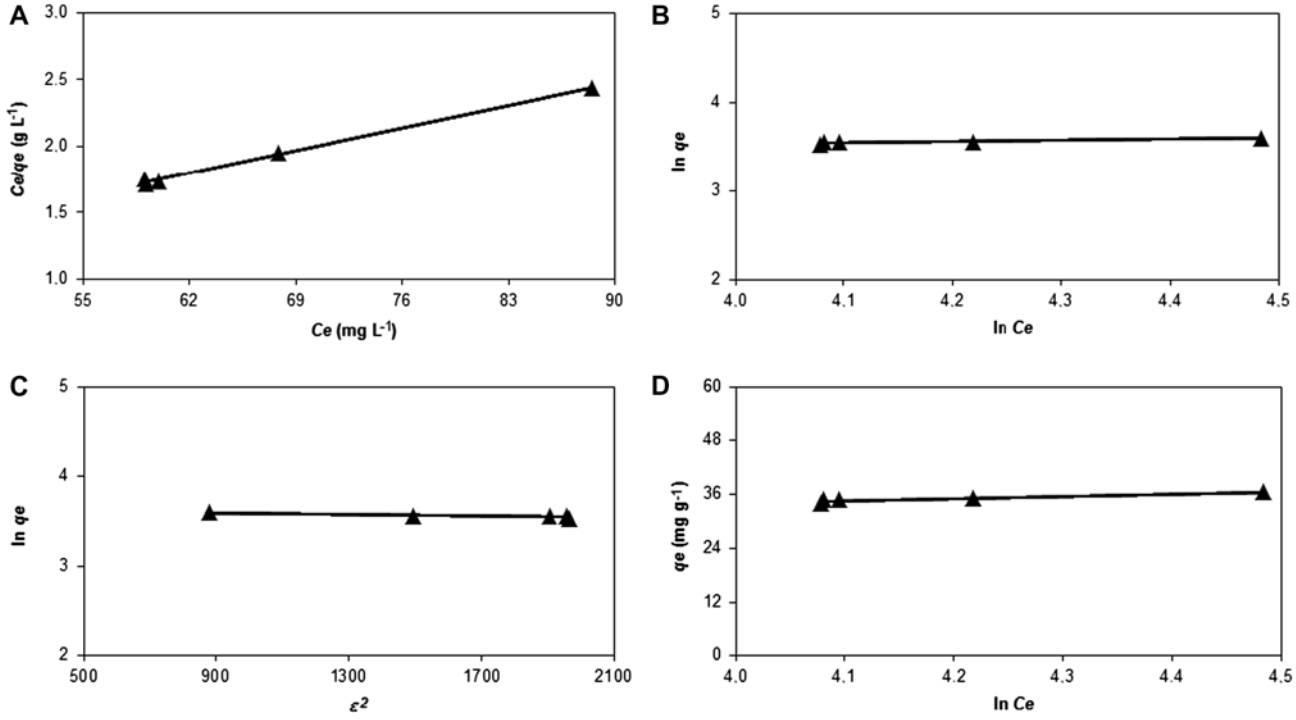

Fig. 10. Plots for (A) Langmuir, (B) Freundlich, (C) D-R and (D) Temkin equilibrium models.

The value of R_L indicates the type of isotherm to be irreversible ($R_L = 0$), favorable ($0 < R_L < 1$), linear ($R_L = 1$) or unfavorable ($R_L > 1$) [3]. The R_L value in this study was found as 0.11 indicating that the adsorption process was favourable.

The Freundlich model can be represented as [17]:

$$\ln q_e = \ln K_f + \frac{1}{n_f} \ln C_e \quad (6)$$

where K_f is the relative adsorption capacity of adsorbent and n_f is a constant related to adsorption intensity. K_f and n_f values can be determined from the slope and intercept of the plots between ln q_e and ln C_e, respectively (Fig. 10(B)). The n_f value was found as 7.19 in the present case. The adsorption process is suitable when the value of n_f is greater than unity [11].

The D-R model can be expressed as [18]:

$$\ln q_e = \ln q_m - B\varepsilon^2 \quad (7)$$

$$\varepsilon = RT \ln\left(1 + \frac{1}{C_e}\right) \quad (8)$$

where B is a constant related to the adsorption energy, ε is the Polanyi potential, R is the universal gas constant (8.314 J mol^{-1}K^{-1}) and T is the absolute temperature. The values of q_m and B are obtained by plotting ln q_e vs. ε^2 (Fig. 10(C)).

The Temkin model can be shown as [19]:

$$q_e = \frac{RT}{b_T} \ln A_T + \frac{RT}{b_T} \ln C_e \quad (9)$$

where A_T and b_T are the Temkin constants. These constants are determined from the slope and intercept of the plot obtained by plotting q_e vs. ln C_e, respectively (Fig. 10(D)). All the calculated parameters of these isotherm models are given in Table 3 (pH: 4, m: 1 g L^{-1}, d_p: 63–125 μm, C_o: 100 mg L^{-1}, T: 45°C and t: 120 min).

Table 3
Equilibrium parameters for LY2R adsorption

Langmuir			
b (L mg^{-1})	q_m (mg g^{-1})	R^2	χ^2
0.08	41.15	0.9963	0.48
Freundlich			
K_f (mg g^{-1})(mg L^{-1})$^{-1/n}$	n_f	R^2	χ^2
19.48	7.19	0.8401	2.06
D-R			
B (mol^2 kJ^{-2})	q_m (mg g^{-1})	R^2	χ^2
0.00005	37.96	0.8254	2.63
Temkin			
A_T (L mg^{-1})	b_T (J mol^{-1})	R^2	χ^2
18.42	538.01	0.8471	1.96

According to the statistical analyses, the adsorption equilibrium data could be well interpreted by the Langmuir isotherm model. This result shows that the LY2R adsorption took place at specific homogeneous sites and a one-layer adsorption onto the PC [20].

3.4. Kinetic studies

The kinetic data provide important information for designing and modelling the adsorption process. Several kinetic models are available to describe the adsorption kinetics. The pseudo-first-order, pseudo-second-order, Elovich and intra-particle diffusion models were applied to the experimental data to evaluate the kinetics of LY2R adsorption by the PC.

The pseudo-first-order kinetic model can be defined as [21]:

$$\frac{1}{q} = \frac{k_1}{q_e t} + \frac{1}{q_e} \tag{10}$$

where k_1 is the pseudo-first-order rate constant. The values of q_e and k_1 can be determined from the slope and intercept of the plot obtained by plotting $1/q$ vs. $1/t$, respectively (Fig. 11(A)).

The pseudo-second-order kinetic model can be represented as [22]:

$$\frac{t}{q} = \frac{1}{k_2 q_e^2} + \frac{t}{q_e} \tag{11}$$

where k_2 is the pseudo-second-order rate constant. The k_2 and q_e are determined from the slope and intercept of the plot of t/q vs. t (Fig. 11(B)).

The Elovich model can be expressed as [23]:

$$q = \frac{1}{\beta}\ln(\alpha\beta) + \frac{1}{\beta}\ln t \tag{12}$$

where α is the initial adsorption rate and β is the desorption constant. A plot of q vs. ln$t$ should yield a linear relationship with a slope of $(1/\beta)$ and an intercept of $1/\beta \ln(\alpha\beta)$ (Fig. 11(C)). The parameters obtained for all the kinetic models are presented in Table 4 (pH: 4, m: 1 g L^{-1}, d_p: 63–125 μm, C_o: 100 mg L^{-1}, T: 45 °C and t: 120 min). As seen from the table, due to the relatively high R^2 as well as small χ^2 values, the pseudo-second-order could be predominant kinetic model for the LY2R adsorption by the PC.

In order to identify the diffusion mechanism, the intra-particle diffusion model can be represented as [24]:

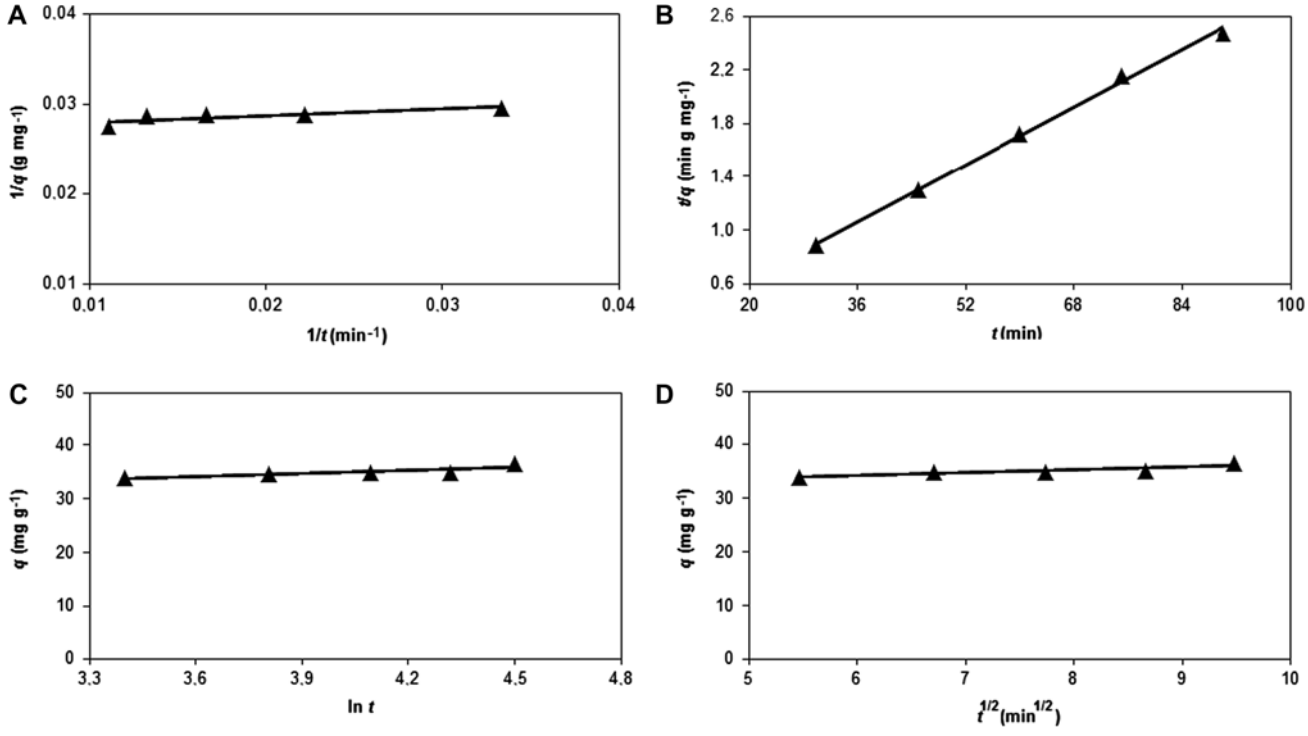

Fig. 11. Plots for (A) pseudo-first-order, (B) pseudo-second-order, (C) Elovich, and (D) intra-particle diffusion kinetic models.

Table 4
Kinetic parameters for LY2R adsorption

Pseudo-first-order			
k_1 (min^{-1})	q_e ($mg\,g^{-1}$)	R^2	χ^2
2.62	36.63	0.7247	4.32
Pseudo-second-order			
k_2 ($g\,mg^{-1}\,min^{-1}$)	q_e ($mg\,g^{-1}$)	R^2	χ^2
0.00744	37.31	0.9977	0.53
Elovich			
α ($mg\,g^{-1}\,min^{-1}$)	β ($g\,mg^{-1}$)	R^2	χ^2
3.93	0.53	0.7774	3.44
Intra-particle diffusion			
k_p ($mg\,g^{-1}\,min^{-1/2}$)	C ($mg\,g^{-1}$)	R^2	χ^2
0.52	30.91	0.8086	2.29

$$q = k_p t^{0.5} + C \quad (13)$$

where k_p is the intra-particle diffusion rate constant and C is a constant which gives information about the thickness of boundary layer. According to this model, the plot of q vs. $t^{0.5}$ yields a straight line passing through the origin if the adsorption process obeys the sole intra-particle diffusion model (Fig. 11(D)). However, it is not the case in the present study. The result showed that this process is complex and may involve more than one mechanism [11,12].

3.5. Thermodynamic analyses

The thermodynamic parameters including the standard Gibbs free energy change (ΔG°), standard enthalpy change (ΔH°) and standard entropy change (ΔS°) for this system can be estimated by the following equations [20]:

$$\Delta G^\circ = -RT \ln K_c \quad (14)$$

$$\ln K_c = -\frac{\Delta H^\circ}{RT} + \frac{\Delta S^\circ}{R} \quad (15)$$

where K_c is the distribution coefficient (C_s/C_e). By plotting ln K_c vs. $1/T$, the values of ΔH° and ΔS° can be determined from the slope and intercept. For current study, the negative ΔG° ($-3.30\,kJ\,mol^{-1}$) suggests that the adsorption of LY2R onto the PC was feasible and spontaneous, thermodynamically. The positive ΔH° ($59.06\,kJ\,mol^{-1}$) proposes that this process is endothermic in nature while the positive ΔS° ($0.26\,kJ\,mol^{-1}\,K^{-1}$) indicates the increased randomness at the solid/liquid interface during the adsorption process [25,26].

4. Conclusions

This study investigated the LY2R removal by the PC from aqueous solutions. The equilibrium data fitted well with the Langmuir isotherm model. The monolayer adsorption capacity of PC was found as $41.15\,mg\,g^{-1}$. The kinetic data were best described by the pseudo-second-order model. Thermodynamic parameters indicated that this adsorption system was spontaneous and endothermic. The results showed that the PC as an eco-friendly and cheap adsorbent could be a suitable alternative for LY2R removal from aqueous media.

References

[1] Z. Aksu, E. Balibek, Effect of salinity on metal-complex dye biosorption by *Rhizopus arrhizus*, J. Environ. Manage. 91 (2010) 1546–1555.
[2] L.N. Du, Y.Y. Yang, G. Li, S. Wang, X.M. Jia, Y.H. Zhao, Optimization of heavy metal-containing dye Acid Black 172 decolorization by *Pseudomonas* sp. DY1 using statistical designs, Int. Biodeter. Biodegrad. 64 (2010) 566–573.
[3] K.Y. Foo, B.H. Hameed, Insights into the modeling of adsorption isotherm systems, Chem. Eng. J. 156 (2010) 2–10.
[4] P. Sharma, H. Kaur, M. Sharma, V. Sahore, A review on applicability of naturally available adsorbents for the removal of hazardous dyes from aqueous waste, Environ. Monit. Assess. 183 (2011) 151–195.
[5] M.E. Fernandez, G.V. Nunell, P.R. Bonelli, A.L. Cukierman, Effectiveness of *Cupressus sempervirens* cones as biosorbent for the removal of basic dyes from aqueous solutions in batch and dynamic modes, Bioresour. Technol. 101 (2010) 9500–9507.
[6] N.M. Mahmoodi, B. Hayati, M. Arami, C. Lan, Adsorption of textile dyes on *Pine Cone* from colored wastewater: Kinetic, equilibrium and thermodynamic studies, Desalination 268 (2011) 117–125.
[7] A.E. Ofomaja, E.B. Naidoo, S.J. Modise, Removal of copper(II) from aqueous solution by pine and base modified pine cone powder as biosorbent, J. Hazard. Mater. 168 (2009) 909–917.
[8] A.E. Ofomaja, E.B. Naidoo, Biosorption of copper from aqueous solution by chemically activated pine cone: A kinetic study, Chem. Eng. J. 175 (2011) 260–270.
[9] A.E. Ofomaja, E.B. Naidoo, Biosorption of lead(II) onto pine cone powder: Studies on biosorption performance and process design to minimize biosorbent mass, Carbohydr. Polym. 82 (2010) 1031–1042.
[10] M.A.M. Salleh, D.K. Mahmoud, W.A.W.A. Karim, A. Idris, Cationic and anionic dye adsorption by agricultural solid wastes: A comprehensive review, Desalination 280 (2011) 1–13.
[11] S. Chowdhury, P. Saha, Sea shell powder as a new adsorbent to remove Basic Green 4 (Malachite Green) from aqueous solutions: Equilibrium, kinetic and thermodynamic studies, Chem. Eng. J. 164 (2010) 168–177.
[12] P.D. Saha, S. Chakraborty, S. Chowdhury, Batch and continuous (fixed-bed column) biosorption of crystal violet by *Artocarpus heterophyllus* (jackfruit) leaf powder, Colloid Surf. B 92 (2012) 262–270.
[13] Y. Safa, H.N. Bhatti, I.A. Bhatti, M. Asgher, Removal of Direct Red-31 and Direct Orange-26 by low cost rice husk: Influence of immobilisation and pretreatments, Can. J. Chem. Eng. 89 (2011) 1554–1565.
[14] M. Greluk, Z. Hubicki, Comparison of the gel anion exchangers for removal of Acid Orange 7 from aqueous solution, Chem. Eng. J. 170 (2011) 184–193.

[15] I. Langmuir, The adsorption of gases on plane surfaces of glass, mica and platinum, J. Am. Chem. Soc. 40 (1918) 1361–1403.
[16] Y. Yang, G. Wang, B. Wang, Z. Li, X. Jia, Q. Zhou, Y. Zhao, Biosorption of Acid Black 172 and Congo Red from aqueous solution by nonviable *Penicillium* YW 01: Kinetic study, equilibrium isotherm and artificial neural network modeling, Bioresour. Technol. 102 (2011) 828–834.
[17] H.M.F. Freundlich, Over the adsorption in solution, J. Phys. Chem. 57 (1906) 385–470.
[18] M.M. Dubinin, L.V. Radushkevich, Equation of the characteristic curve of activated charcoal, Proc. Acad. Sci. USSR 55 (1947) 331–333.
[19] M.J. Temkin, V. Pyzhev, Kinetics of ammonia synthesis on promoted iron catalysts, Acta Physiochim. URSS 12 (1940) 217–222.
[20] H.B. Senturk, D. Ozdes, C. Duran, Biosorption of Rhodamine 6G from aqueous solutions onto almond shell (*Prunus dulcis*) as a low cost biosorbent, Desalination 252 (2010) 81–87.
[21] Z. Bekçi, Y. Seki, L. Cavas, Removal of malachite green by using an invasive marine alga *Caulerpa racemosa* var. *cylindracea*, J. Hazard. Mater. 161 (2009) 1454–1460.
[22] Y.S. Ho, G. McKay, Pseudo-second-order model for sorption processes, Process Biochem. 34 (1999) 451–465.
[23] S.H. Chien, W.R. Clayton, Application of Elovich equation to the kinetics of phosphates release and sorption in soils, Soil Sci. Soc. Am. J. 44 (1980) 265–268.
[24] W.J. Weber, J.C. Morris, Kinetics of adsorption on carbon from solution, J. Sanit. Eng. Div. ASCE 89 (1963) 31–60.
[25] N.M. Mahmoodi, B. Hayati, M. Arami, Kinetic, equilibrium and thermodynamic studies of ternary system dye removal using a biopolymer, Ind. Crops Prod. 35 (2012) 295–301.
[26] Y. Feng, F. Yang, Y. Wanga, L. Ma, Y. Wua, P.G. Kerr, L. Yang, Basic dye adsorption onto an agro-based waste material – Sesame hull (*Sesamum indicum* L.), Bioresour. Technol. 102 (2011) 10280–10285.